THE JOURNAL OF PHYSICAL CHEMISTRY C

ARTICLE

pubs.acs.org/JPCC

# Self-Limiting Film Growth of Transparent Conducting $In_2O_3$ by Atomic Layer Deposition using Trimethylindium and Water Vapor

Do-Joong Lee,[†] Jang-Yeon Kwon,[†] Jae Il Lee,[‡,§] and Ki-Bum Kim[†,‡,§,*]

[†]Department of Materials Science and Engineering, Seoul National University, Seoul 151-742, Korea

[‡,§]WCU Hybrid Materials Program, Department of Materials Science and Engineering, Seoul National University, Seoul 151-742, Korea

**ABSTRACT:** Conformal and self-limiting film growth of transparent conducting $In_2O_3$ is demonstrated with atomic layer deposition (ALD) using trimethylindium (TMIn) and water vapor. Various parameters, including pulsing times of TMIn and $H_2O$ and deposition temperature, are varied to confirm the ALD processing window of $In_2O_3$. It is found that an extremely large Langmuir exposure of $H_2O$ (~2 Torr s) is required to fully react the surface-adsorbed In-$(CH_3)$* groups with $H_2O$. Self-limiting film growth is obtainable at the deposition temperatures between 200 and 251 °C where the film growth is controlled by surface adsorption of TMIn molecules. Within the ALD window, ALD-$In_2O_3$ exhibits a film growth rate of ~0.039 nm/cycle at 217 °C. In addition, the film exhibits an excellent step coverage of ~97% on a high-aspect-ratio (~11) nanostructure. The resistivity of the ALD-$In_2O_3$ film deposited at 200 °C is about $2.8 \times 10^{-3}$ Ω cm, and this is attributed to the high Hall mobility of 84 $cm^2/(V\,s)$. Finally, the reduction of the Hall mobility of the films with respect to increases in the deposition temperature is correlated to the evolution of microstructures.

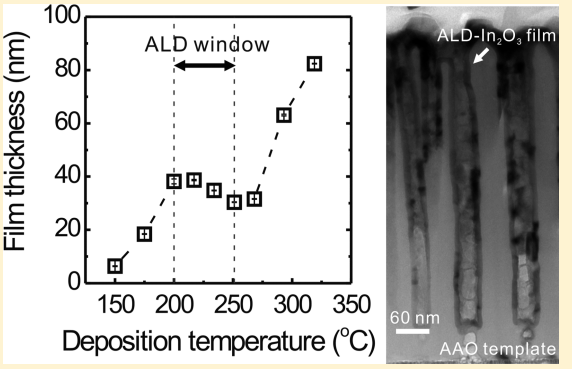


## 1. INTRODUCTION

$In_2O_3$ has been widely investigated for various applications such as photovoltaic devices, electrochemical sensors, and flat panel displays.[1−3] For instance, intrinsic or Sn-doped $In_2O_3$ (ITO) have been extensively employed as transparent electrodes due to their low resistivity (~$10^{-4}$ Ω cm) and high transmittance of the visible rays (>80%).[4,5] In addition, $In_2O_3$ is a major component of high-mobility amorphous oxides, such as Ga−In−Zn−O and Hf−In−Zn−O, for thin film transistors.[1,6−9] For those applications, $In_2O_3$ has been typically deposited using sputtering, evaporation, chemical vapor deposition (CVD), or a sol−gel process.[4,5,10,11] Recently, atomic layer deposition (ALD) has been considered as a potential deposition method of $In_2O_3$.[12−17] Due to the surface-saturated reaction mechanism, ALD allows conformal film deposition on large area substrates.[18] This particular aspect gives ALD-$In_2O_3$ films their potential to be utilized in emerging applications, such as nanostructured solar cells.[19,20]

There have been many efforts to obtain conformal ALD-$In_2O_3$ films using various precursors including $InCl_3$,[12,13] β-diketonates [$In(hfac)_3$ (hfac: hexafluoroacetylacetonate)[13,15] and $In(acac)_3$ (acac: acetylacetonate)[14,15]], InCp (Cp: cyclopentadienyl),[15] and TMIn (trimethyl indium).[13,16,17] Initially, $InCl_3$ and $H_2O$ were tested as a precursor and a reactant, respectively, for the ALD of $In_2O_3$.[12,13] Even though they could obtain an $In_2O_3$ film at a high deposition temperature above 400 °C, that system suffered from the films being etched by HCl byproducts and thereby conformal film deposition onto high-aspect-ratio structures was inhibited. When β-diketonates were introduced with $H_2O$ or ozone reactants, a very low film growth rate (<0.03 nm/cycle) was obtained in a temperature range of 165−225 °C, probably due to poor adsorption of the precursors on the $In_2O_3$ surface.[13−15] Recently, conformal ALD of $In_2O_3$ films has been demonstrated using InCp.[15] In that report, the combination of InCp/ozone resulted in relatively high film growth rates of 0.13−0.2 nm/cycle at deposition temperatures in the range of 200−450 °C, while there was negligible film growth with other oxidants including water and oxygen. However, the use of ozone as a strong oxidant has potential issues such as oxidation of underlying substrates and the necessity of complicated equipment.[21] In addition, it was reported that ALD-$In_2O_3$ films deposited using ozone have higher film resistivity (>$10^{-2}$ Ω cm), owing to the removal of native donors, such as oxygen vacancies ($V_o^{2+}$) and interstitial In ($In_i^{3+}$).[14,15] Therefore, an ozone-free ALD-$In_2O_3$ process is still necessary for transparent electrode applications, and this will be accomplished by the investigation of other precursors and/or reactants.

Among the various precursors, TMIn has several advantages, including a simple chemical structure and a high vapor pressure (~1.7 Torr at room temperature).[22] In addition, TMIn is one of the most utilized commercial precursors and has been extensively studied for CVD and ALD of various In-compounds.[23−25] Despite these advantages, there have been no accomplishments with respect to self-limiting ALD-$In_2O_3$ using the TMIn precursor. In the case of TMIn/hydrogen peroxide ($H_2O_2$), it

**Received:** March 15, 2011
**Revised:** June 22, 2011
**Published:** June 27, 2011





dx.doi.org/10.1021/jp2024389 | J. Phys. Chem. C 2011, 115, 15384–15389

was reported that overall film growth occurred due to the thermal decomposition of TMIn at a high deposition temperature (>300 °C), while no film growth was observed below that temperature.[16] There have also been two contradictory reports that utilized water vapor. First, Ritala et al. obtained no film growth using TMIn/$H_2O$ even though the detailed deposition conditions were not specified.[13] In contrast, Ott et al. observed an extremely high film growth rate (>1 nm/cycle) at 252 °C due to the pyrolysis of TMIn.[17] Inconsistently at the same temperature, they confirmed that the TMIn/$H_2O$ system undergoes a typical binary reaction consisting of the adsorption of TMIn onto surface −OH groups and the subsequent reaction of those with $H_2O$, and this was confirmed using in situ Fourier transform infrared (FTIR) spectroscopy in a different apparatus. This observation is even contrary to their ALD results, probably due to the different calibration temperature. As described in these examples, the reports of ALD-$In_2O_3$ using TMIn have shown no consensus and efforts to optimize deposition conditions are still lacking.

In this work, we report conformal and self-limiting film growth of ALD-$In_2O_3$ using a TMIn precursor and $H_2O$ reactant though the optimization of various processing parameters, including the deposition temperature and pulsing times of TMIn and $H_2O$. Specifically, we report that the amount of $H_2O$ exposure is one of the key factors determining the ALD process. Film conformality of ALD-$In_2O_3$ was confirmed by depositing a film onto a high-aspect-ratio anodized aluminum oxide (AAO) template. Finally, the electrical properties, including resistivity, Hall mobility and carrier concentration were studied using Hall measurements and those were explained in terms of film microstructures.

## 2. EXPERIMENTAL SECTION

$In_2O_3$ films were deposited on Si (for thickness measurement) or $SiO_2$ (100 nm)/Si substrates (for Hall measurement) using a traveling-wave type ALD system (Lucida D-100, NCD Technology, Korea) with a temperature range of 150−329 °C. TMIn (UP Chemical Co., Ltd., Korea) and $H_2O$ were introduced as a precursor and reactant, respectively. The temperature of a TMIn canister was maintained at 20 °C and a $H_2O$ canister was held at room temperature. Injection of the TMIn was supported by the $N_2$ boost system. During the $H_2O$ exposure, an increase of the chamber pressure was about 600−700 mTorr. One ALD cycle consisted of TMIn pulsing−$N_2$ purge (10 s)−$H_2O$ pulsing−$N_2$ purge (10 s) where the pulsing times of TMIn and $H_2O$ were varied. Film thickness was measured using ellipsometry (wavelength: 632.8 nm). Film conformality was checked by depositing films onto the AAO template (width: 49 nm, length: 540 nm) formed on a $SiO_2$ (100 nm)/Si substrate. During the anodization, oxalic acid was used as an electrolyte and the bias and temperature were maintained at 40 V and 10 °C, respectively.[26,27] The electrical properties were investigated using a Hall measurement system (BIO-RAD, HL5500PC) with the Van der Pauw configuration. Microstructures of the ALD-$In_2O_3$ films were observed by transmission electron microscopy (TEM, JEOL, JEM-3000F).

## 3. RESULTS AND DISCUSSION

To study the film deposition characteristics of ALD-$In_2O_3$, various parameters, including deposition temperature and pulsing times of TMIn and $H_2O$, were varied. Figure 1 shows the thickness of $In_2O_3$ films deposited for 1000 ALD cycles as a function of TMIn pulsing time. The deposition temperature was also varied from 217 to 293 °C, while the $H_2O$ pulsing time was fixed at 1 s. In Figure 1, the film thickness remained almost constant as the TMIn pulsing time increased (≥1 s) when the deposition temperature was below 251 °C. This indicates that the film growth is self-limiting in that temperature range as is typically exhibited in ALD-films. Interestingly, this result is quite different compared to the results of previous reports that showed either uncontrolled film deposition owing to the thermal decomposition of TMIn or no film growth.[13,17] In contrast, at temperatures above 251 °C, the film thickness gradually increased as the TMIn pulsing time increased.

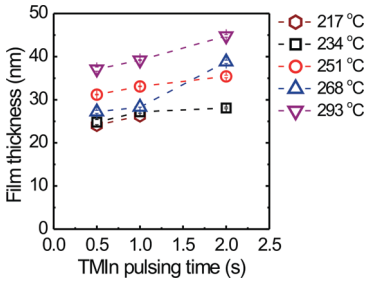


**Figure 1.** Thickness of ALD-$In_2O_3$ films as a function of TMIn pulsing time. All films were deposited for 1000 ALD cycles. Pulsing time of the $H_2O$ was fixed at 1 s.

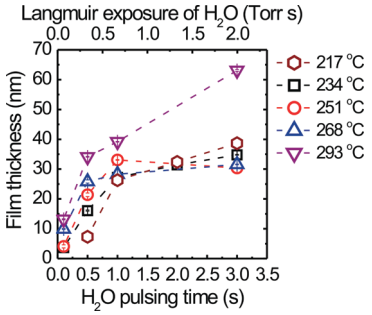


**Figure 2.** Thickness of ALD-$In_2O_3$ films as a function of $H_2O$ pulsing time. All films were deposited for 1000 ALD cycles. Pulsing time of the TMIn was fixed at 1 s.

Second, the pulsing time of $H_2O$ was varied to further optimize the ALD-$In_2O_3$ process. Figure 2 shows the thickness of ALD-$In_2O_3$ films deposited for 1000 cycles as a function of $H_2O$ pulsing time. Herein, the TMIn pulsing time was constant at 1 s. Interestingly, in Figure 2, the film thickness increased drastically as the $H_2O$ pulsing time was extended to 3 s. For example, the film thickness increased from 7 to 39 nm at 217 °C by increasing the $H_2O$ pulsing time from 0.5 to 3 s. This result indicates that an extremely large Langmuir exposure of $H_2O$ (~2 Torr s) was required for the complete conversion of surface-adsorbed In-$(CH_3)$* groups to In−OH* groups. This exposure is much higher than that of the previous report using a $H_2O_2$ reactant (~0.002 Torr s), which resulted in no film growth below 300 °C.[16] In addition, it is quite contrary to other ALD-oxides which require a relatively small $H_2O$ exposure of ≤0.1 Torr s.[28] For example, in the same equipment, the saturation behavior was observed even at the $H_2O$ exposure of ~0.07 Torr s for ALD of ZnO [diethyl zinc (DEZn)], $HfO_2$ [tetrakis(ethylmethylamido) hafnium (TEMAHf)], and $TiO_2$ [titanium tetrakisisopropoxide (TTIP)] (data not shown). Therefore, these results indicate that

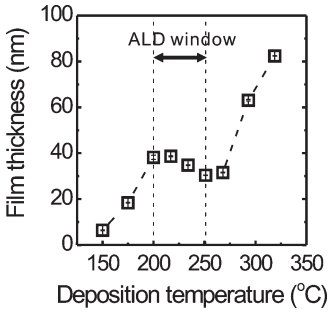


**Figure 3.** Thickness of the ALD-$In_2O_3$ films deposited for 1000 ALD cycles with respect to the deposition temperature. ALD sequence was TMIn 1 s−purge 10 s−$H_2O$ 3 s−purge 10 s. Arrowed region indicates an ALD window which exhibits the self-limiting film growth.

the reaction kinetics of the In-$(CH_3)$* groups with $H_2O$ are much slower than those of other metal−organic precursors. For example, Ott et al. and Dillon et al. conducted in situ FTIR study during the ALD of $In_2O_3$ (TMIn/$H_2O$) and $Al_2O_3$ [TMA (trimethylaluminum)/$H_2O$].[17,29] They found that the $H_2O$ exposure required for the conversion of In-$(CH_3)$* groups to In-(OH)* groups was more than 200 times larger compared to that of Al-$(CH_3)$* groups. These reports clearly support the idea that a considerably large $H_2O$ exposure is necessary in the TMIn/$H_2O$ system due to the poor reactivity between surface-adsorbed In-$(CH_3)$* groups and $H_2O$ even though it is still unclear whether that reaction is thermodynamically less probable or has a high activation energy.

Figure 3 shows the thickness of the ALD-$In_2O_3$ films deposited at various temperatures. Herein, all films were deposited for 1000 ALD cycles and pulsing times of the TMIn and $H_2O$ were 1 and 3 s, respectively. As evident in Figure 3, there are three distinct regimes of the film thickness with respect to the deposition temperature. First, at low deposition temperature regime below 200 °C, the film thickness drastically increased as the temperature increased. This indicates that the film growth is determined by the thermal activation of either the adsorption of TMIn or the reaction of surface-adsorbed species with $H_2O$. Meanwhile, in the intermediate temperature regime between 200 and 251 °C, the film thickness gradually decreased as the deposition temperature increased (for instance, from 38 nm at 200 °C to 30 nm at 251 °C). Interestingly, this decrease corresponds to the decrease of −OH groups on the ALD-$In_2O_3$ surface with respect to the temperature, as reported by the in situ FTIR study.[17] Therefore, it is believed that the film growth in that regime is self-limiting as controlled by the adsorption of TMIn onto the surface −OH groups rather than by the reaction kinetics between the In-$(CH_3)$* groups and $H_2O$. In contrast, when the deposition temperature is above 251 °C, the film thickness increased abruptly as the temperature increased. In addition, as previously shown in Figure 1, the film thickness increased with increasing the TMIn pulsing time at the same deposition temperatures. This means that the self-limiting film growth was inhibited by the thermal decomposition of TMIn, which was also observed at a similar temperature range (>252 °C) in the previous report.[17] Therefore, it is clear that the self-limiting film growth of ALD-$In_2O_3$ using TMIn/$H_2O$ can be obtainable between 200 and 251 °C by rigorously selecting the process parameters.

Figure 4a shows the thickness of the ALD-$In_2O_3$ films as a function of the number of ALD cycles. Herein, the deposition

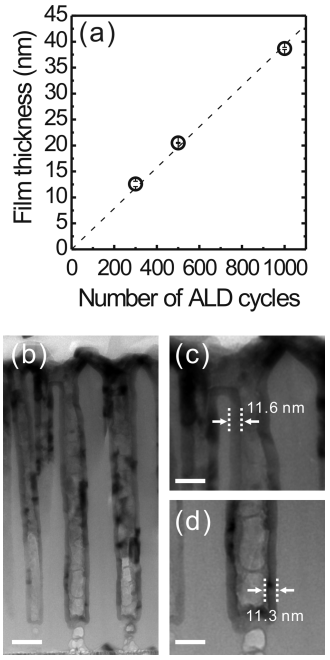


**Figure 4.** (a) Film thickness of the ALD-$In_2O_3$ films as a function of the number of ALD cycles. ALD sequence was TMIn 1 s−purge 10 s−$H_2O$ 3 s−purge 10 s and the deposition temperature was 217 °C. (b) Cross-sectional view TEM micrograph of an AAO template coated with ALD-$In_2O_3$ films for 300 ALD cycles. Parts (c) and (d) are magnified images of the top and bottom of the AAO walls in (b), respectively. Scale bar indicates 60 nm for (b) and 30 nm for (c) and (d), respectively.

temperature was 217 °C and the pulsing times of the TMIn and $H_2O$ were set to 1 and 3 s, respectively. As clearly shown in Figure 4a, the film thickness was linear with respect to the number of ALD cycles. This result also indicates that the ALD-$In_2O_3$ process in this study is self-limiting. The film growth rate obtained from the linear fitting was about ∼0.039 nm/cycle, which is slightly higher than that of $InCl_3$ and $\beta$-diketonates (<0.03 nm/cycle).[12−14] By using this deposition condition, film conformality was confirmed by depositing films onto a high-aspect-ratio nanostructure. Figure 4b−d show cross-sectional view TEM micrographs of an ALD-$In_2O_3$ film deposited for 300 ALD cycles onto an AAO template (aspect ratio: ∼11). In Figure 4b, it is clear that the $In_2O_3$ film, visualized as the dark contrast, was uniformly coated on the walls of the template. The average film thickness was about ∼11.6 nm on the top part of the holes (Figure 4c) and ∼11.3 nm on the bottom (Figure 4d), which results in a high step coverage of ∼97%. This result clearly represents the ability of the conformal ALD-$In_2O_3$ coating onto high-aspect-ratio structures using the TMIn/$H_2O$.

For the application of transparent electrodes, electrical properties of the ALD-$In_2O_3$ films were investigated using Hall measurements. Figure 5 shows resistivity of the ALD-$In_2O_3$ films as a function of the deposition temperature. Herein, all films were deposited using the ALD sequence of TMIn 1 s−purge 10 s−$H_2O$ 3 s−purge 10 s and the film thickness was set to 30−40 nm. As shown in Figure 5, the film resistivity exhibited values between $2.8 \times 10^{-3}$ Ω cm and $5.0 \times 10^{-3}$ Ω cm at the deposition temperatures of 200−329 °C. These values are similar or much lower than the ALD-$In_2O_3$ films deposited using other precursors [$1.6 \times 10^{-2}$ Ω cm for InCp/$O_3$, $3 \times 10^{-2}$−60 Ω cm for In(acac)$_3$/$H_2O$, and $(3 - 6) \times 10^{-3}$ Ω cm for $InCl_3$/$H_2O$].[12,14,15] However, the


dx.doi.org/10.1021/jp2024389 |J. Phys. Chem. C 2011, 115, 15384–15389

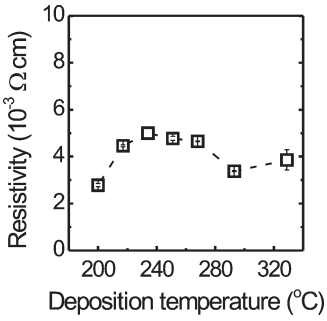


**Figure 5.** Resistivity of the ALD-$In_2O_3$ films deposited at various temperatures with the thickness of 30−40 nm. ALD sequence was TMIn 1 s−purge 10 s−$H_2O$ 3 s−purge 10 s.

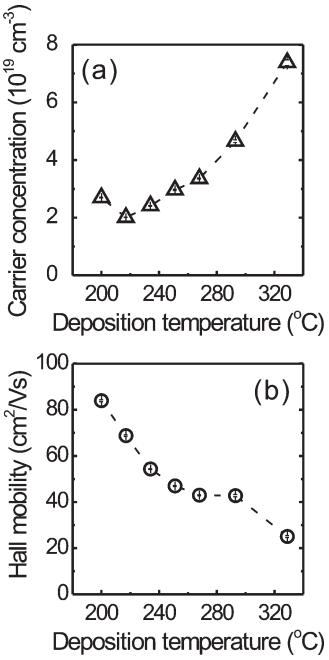


**Figure 6.** (a) Carrier concentration and (b) Hall mobility of the ALD-$In_2O_3$ films deposited at various temperatures.

film resistivity of ALD-$In_2O_3$ in this work was relatively higher than that of the films deposited by sputtering, evaporation, or PLD ($10^{-4}$−$10^{-3}$ Ω cm).[4,10,30−33]

The carrier concentration and the Hall mobility of those ALD-$In_2O_3$ films were further studied. Figure 6a shows the carrier concentration of the ALD-$In_2O_3$ films deposited at various temperatures. As the temperature increased from 200 to 329 °C, the carrier concentration increased from 2.7 × $10^{19}$ $cm^{-3}$ to 7.4 × $10^{19}$ $cm^{-3}$. For example, in terms of the grain boundary trapping, a carrier concentration can be higher when a grain size is larger. However, this explanation cannot be applied to the ALD-$In_2O_3$ films because the grain size becomes smaller as increasing the deposition temperature, which will be discussed in Figure 7. Otherwise, as the deposition temperature increases, the equilibrium vapor pressure of oxygen in the $In_2O_3$ films increases thermodynamically and thereby this leads to the formation of oxygen deficient films more readily. Therefore, it is thought that the increase of the carrier concentration in Figure 6a is mainly attributed to the increase of native donors, such as such as $V_o^{2+}$ and $In_i^{3+}$.[34] Meanwhile, the carrier concentration obtained

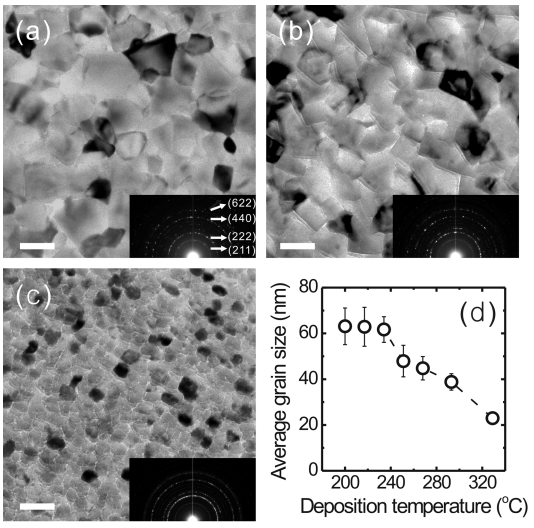


**Figure 7.** Plan-view bright-field TEM micrographs of the ALD-$In_2O_3$ films deposited at (a) 200 °C, (b) 251 °C, and (c) 329 °C. Scale bar indicates 50 nm. Inset figures indicate the selected-area electron diffraction patterns. (d) Average grain size of the ALD-$In_2O_3$ films measured from the plan-view TEM images as a function of the deposition temperature.

in this work was about one order lower compared to the films deposited by other methods, including sputtering and evaporation [(1−5) × $10^{20}$ $cm^{-3}$].[10,30−32] In contrast to the carrier concentration, the Hall mobility of the ALD-$In_2O_3$ films decreased as the deposition temperature increased as shown in Figure 6b. At 200 °C, the Hall mobility was the highest at 84 $cm^2$/(V s). This value is comparable or much higher than the $In_2O_3$ films deposited by ALD using other precursors (~70 $cm^2$/(V s) for $InCl_3/H_2O$ and ~25 $cm^2$/(V s) for InCp/$O_3$)[12,35] or those deposited by other methods (~70 $cm^2$/(V s) for an evaporation, 40−50 $cm^2$/(V s) for a sputtering, and 6−21 $cm^2$/(V s) for a sol−gel process).[10,11,30−32,36] Interestingly in Figure 6b, the Hall mobility decreased continuously to 25 $cm^2$/(V s) as the deposition temperature increased to 329 °C.

Finally, in order to comprehend the change of the Hall mobility with respect to the deposition temperature, microstructures of the ALD-$In_2O_3$ films were investigated using TEM. Figure 7a−c shows bright-field plan-view TEM micrographs of the $In_2O_3$ films deposited at (a) 200 °C, (b) 251 °C, and (c) 329 °C. All films were polycrystalline with the bixbyite structure as confirmed by the electron diffraction patterns (inset figures) and the X-ray diffraction patterns (not shown here).[4] However, those films have considerably different grain sizes. As shown in Figure 7d, the average grain size of the ALD-$In_2O_3$ films, which was measured from the plan-view TEM images by the linear intercept technique, decreased gradually from 63 to 23 nm as increasing the deposition temperature from 200 to 329 °C. Surprisingly, this result indicates that the ALD-$In_2O_3$ film deposited at a higher temperature has a smaller grain size. This is contrary to the cases of $In_2O_3$ films deposited by sputtering or CVD or even other materials deposited by ALD, which show improved crystallinity as the deposition temperature increases.[37−41] Typically, a grain size of a thin film is determined by various factors such as a nucleation rate and a grain growth rate. In the case of the ALD-$In_2O_3$ films, the smaller grain size at higher deposition temperatures might indicate that a nucleation rate becomes higher with increasing the deposition

temperature due to either increase of adatom supply or decrease of activation energy for the nucleation. For instance, the film growth rate of the ALD-$In_2O_3$ films increases above 251 °C with increasing the deposition temperature and thus this would bring about the increase of the nucleation rate due to the increase of deposited monomers. Therefore, it can be imagined that the ALD-$In_2O_3$ films deposited at high temperature could have smaller grain sizes as presented in Figure 7, while further study is necessary to understand the origin of the microstructure evolution with respect to the deposition temperature more clearly. Those results also suggest that the films deposited at higher temperatures have more grain boundaries which act as scattering centers of free electrons. For instance, it is generally known that mobility that is dominated by grain boundary scattering ($\mu_G$) can be expressed as follows:

$$\mu_G = Lq\left(\frac{1}{2\pi m^* k_B T}\right)^{1/2} \exp\left(-\frac{E_b}{k_B T}\right) \quad (1)$$

where $L$ is the grain size, $q$ is the unit charge, $m^*$ is the effective mass of an electron, $k_B$ is the Boltzmann constant, $T$ is the measurement temperature, and $E_b$ is the barrier height at the grain boundaries.[42,43] This equation simply explains that $\mu_G$ is proportional to the grain size $L$. Therefore, it is strongly believed that the higher Hall mobilities of the ALD-$In_2O_3$ films deposited at lower temperatures is attributed to the larger grain sizes of those films.

## 4. CONCLUSIONS

The conformal and self-limiting film growth of ALD-$In_2O_3$ was demonstrated using a TMIn precursor and $H_2O$ reactant. In this study, we found that an extremely large Langmuir exposure of $H_2O$ (~2 Torr s) was required to fully convert surface-adsorbed In-$(CH_3)$* groups to In-(OH)* groups. The film growth of the ALD-$In_2O_3$ at the deposition temperatures between 200 and 251 °C was self-limiting as controlled by the surface-adsorption of TMIn, while it was controlled by the thermal decomposition of TMIn above 251 °C. Within the ALD window, a film growth rate of ~0.039 nm/cycle was obtained at 217 °C. In addition, the films deposited onto the high-aspect-ratio (~11) AAO template exhibited an excellent step coverage of ~97%. The ALD-$In_2O_3$ film deposited at 200 °C had the resistivity of $2.8 \times 10^{-3}$ Ω cm that was attributed to a high Hall mobility of 84 $cm^2/(V\ s)$. Finally, the deposition temperature dependence of the Hall mobility was explained in terms of the grain size of the films.

## AUTHOR INFORMATION

### Corresponding Author

*Phone: 82-2-880-7095; Fax: 82-2-885-5820; E-mail: kibum@snu.ac.kr.

## ACKNOWLEDGMENT

This research was supported by a Basic Science Research Program through the National Research Foundation of Korea (NRF) funded by the Ministry of Education, Science and Technology (2010-0023309). This research was also supported by WCU (World Class University) program through National Research Foundation of Korea funded by the Ministry of Education, Science and Technology (R31-2008-000-10075-0).

## REFERENCES

(1) Nomura, K.; Ohta, H.; Takagi, A.; Kamiya, T.; Hirano, M.; Hosono, H. *Nature* **2004**, *432*, 488.
(2) Granqvist, C. G. *Adv. Mater.* **2003**, *15*, 1789.
(3) Li, C.; Zhang, D.; Liu, X.; Han, S.; Tang, T.; Han, J.; Zhou, C. *Appl. Phys. Lett.* **2003**, *82*, 1613.
(4) Tahar, R. B. H.; Ban, T.; Ohya, Y.; Takahashi, Y. *J. Appl. Phys.* **1998**, *83*, 2631.
(5) Minami, T. *Semicond. Sci. Technol.* **2005**, *20*, S35.
(6) Kamiya, T.; Nomura, K.; Hosono, H. *J. Disp. Technol.* **2009**, *5*, 273.
(7) Kwon, J. Y.; Son, K. S.; Jung, J. S.; Kim, T. S.; Ryu, M. K.; Park, K. B.; Yoo, B. W.; Kim, J. W.; Lee, Y. G.; Park, K. C.; Lee, S. Y.; Kim, J. M. *IEEE Electron Device Lett.* **2008**, *29*, 1309.
(8) Kim, C.-J.; Kim, S.; Lee, J.-H.; Park, J.-S.; Kim, S.; Park, J.; Lee, E.; Lee, J.; Park, Y.; Kim, J. H.; Shin, S. T.; Chung, U.-I. *Appl. Phys. Lett.* **2009**, *95*, 252103.
(9) Kwon, J.-Y.; Lee, D.-J.; Kim, K.-B. *Electron. Mater. Lett.* **2011**, *7*, 1.
(10) Mizuhashi, M. *Thin Solid Films* **1980**, *70*, 91.
(11) Tahar, R. B. H.; Ban, T.; Ohya, Y.; Takahashi, Y. *J. Appl. Phys.* **1997**, *82*, 865.
(12) Asikainen, T.; Ritala, M.; Leskelä, M. *J. Electromchem. Soc.* **1994**, *141*, 3210.
(13) Ritala, M.; Asikainen, T.; Leskelä, M.; Skarp, J. *Mater. Res. Soc. Symp. Proc.* **1996**, *426*, 513.
(14) Nilsen, O.; Balasundaraprabhu, R.; Monakhov, E. V.; Muthukumarasamy, N.; Fjellvåg, H.; Svensson, B. G. *Thin Solid Films* **2009**, *517*, 6320.
(15) Elam, J. W.; Martinson, A. B. F.; Pellin, M. J.; Hupp, J. T. *Chem. Mater.* **2006**, *18*, 3571.
(16) Ozasa, K.; Ye, T.; Aoyagi, Y. *J. Vac. Sci. Technol. A* **1994**, *12*, 120.
(17) Ott, A. W.; Johnson, J. M.; Klaus, J. W.; George, S. M. *Appl. Surf. Sci.* **1997**, *112*, 205.
(18) George, S. M. *Chem. Rev.* **2010**, *110*, 111.
(19) Martinson, A. B. F.; Elam, J. W.; Liu, J.; Pellin, J.; Marks, T. J.; Hupp, J. T. *Nano Lett.* **2008**, *8*, 2862.
(20) Kim, H.; Lee, H.-B.-R.; Maeng, W.-J. *Thin Solid Films* **2009**, *517*, 2563.
(21) Kim, H. *J. Vac. Sci. Technol. B* **2003**, *21*, 2231.
(22) Shenai-Khatkhate, D. V.; DiCarlo, R. L., Jr.; Ware, R. A. *J. Cryst. Growth* **2008**, *310*, 2395.
(23) Wang, C. Y.; Cimalla, V.; Romanus, H.; Kups, T.; Niebelschütz, M.; Ambacher, O. *Thin Solid Films* **2007**, *515*, 6611.
(24) Baucom, K. C.; Biefeld, R. M. *Appl. Phys. Lett.* **1994**, *64*, 3021.
(25) Jeong, W. G.; Menu, E. P.; Dapkus, P. D. *Appl. Phys. Lett.* **1989**, *55*, 244.
(26) Lee, D.-J.; Yim, S.-S.; Kim, K.-S.; Kim, S.-H.; Kim, K.-B. *Electrochem. Solid-State Lett.* **2008**, *11*, K61.
(27) Park, S.-H.; Kim, S.; Lee, D.-J.; Yun, S.; Khim, Z. G.; Kim, K.-B. *J. Electochem. Soc.* **2009**, *156*, K181.
(28) Groner, M. D.; Elam, J. W.; Fabreguette, F. H.; George, S. M. *Thin Solid Films* **2002**, *413*, 186.
(29) Dillon, A. C.; Ott, A. W.; Way, J. D.; George, S. M. *Surf. Sci.* **1995**, *322*, 230.
(30) Minami, T.; Sonohara, H.; Kakumu, T.; Takata, S. *Jpn. J. Appl. Phys.* **1995**, *34*, L971.
(31) Minami, T.; Kakumu, T.; Takeda, Y.; Takata, S. *Thin Solid Films* **1998**, *317*, 326.
(32) Pan, C. A.; Ma, T. P. *Appl. Phys. Lett.* **1980**, *37*, 163.
(33) Tarsa, E. J.; English, J. H.; Speck, J. S. *Appl. Phys. Lett.* **1993**, *62*, 2332.
(34) Leny, S.; Zunger, A. *Phys. Rev. Lett.* **2007**, *98*, 045501.
(35) Elam, J. W.; Baker, D. A.; Martinson, A. B. F.; Pellin, M. J.; Hupp, J. T. *J. Phys. Chem. C* **2008**, *112*, 1938.
(36) Takahashi, Y.; Hayashi, H.; Ohya, Y. *Mater. Res. Soc. Symp. Proc.* **1992**, *271*, 401.
(37) Meng, L.-j.; dos Santos, M. P. *Thin Solid Films* **1998**, *322*, 56.

(38) Wang, C.; Cimalla, V.; Cherkashinin, G.; Romanus, H.; Ali, N.; Ambacher, O. *Thin Solid Films* **2007**, *515*, 2921.
(39) Kim, N. H.; Myung, J. H.; Kim, H. W.; Lee, C. *Phys. Stat. Sol. A* **2005**, *202*, 108.
(40) Choi, S.-H.; Cheon, T.; Kim, S.-H.; Kang, D.-H.; Park, G.-S.; Kim, S. *J. Electrochem. Soc.* **2011**, *158*, D351.
(41) Hämäläinen, J.; Kemell, M.; Munnki, F.; Kreissig, U.; Ritala, M.; Leskelä, M. *Chem. Mater.* **2008**, *20*, 2903.
(42) Seto, J. Y. W. *J. Appl. Phys.* **1975**, *46*, 5247.
(43) Ellmer, K.; Mientus, R. *Thin Solid Films* **2008**, *516*, 4620.